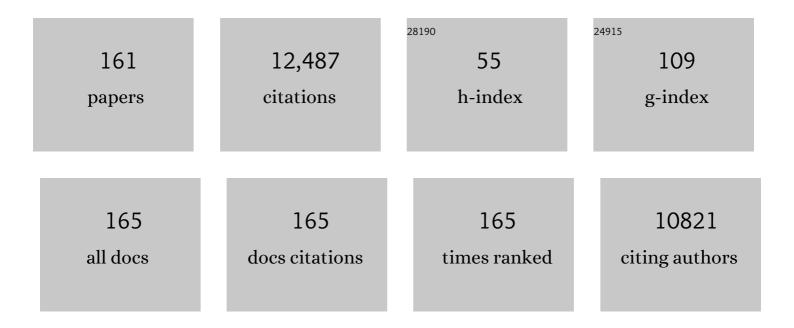
## Qing Shen

List of Publications by Year in descending order

Source: https://exaly.com/author-pdf/1609401/publications.pdf Version: 2024-02-01



OINC SHEN

#	Article	IF	CITATIONS
1	Large synergy effects of doping, a site substitution, and surface passivation in wide bandgap Pb-free ASnI2Br perovskite solar cells on efficiency and stability enhancement. Journal of Power Sources, 2022, 520, 230848.	4.0	13
2	Exponential optical absorption edge in PbS quantum dot-ligand systems on single crystal rutile-TiO <sub>2</sub> revealed by photoacoustic and absorbance spectroscopies. Materials Research Express, 2022, 9, 025005.	0.8	1
3	Tin–Lead Perovskite Solar Cells Fabricated on Hole Selective Monolayers. ACS Energy Letters, 2022, 7, 966-974.	8.8	111
4	High performance wide bandgap Lead-free perovskite solar cells by monolayer engineering. Chemical Engineering Journal, 2022, 436, 135196.	6.6	33
5	Enhanced efficiency and stability in Sn-based perovskite solar cells by trimethylsilyl halide surface passivation. Journal of Energy Chemistry, 2022, 71, 604-611.	7.1	19
6	Enhancing the Electronic Properties and Stability of High-Efficiency Tin–Lead Mixed Halide Perovskite Solar Cells via Doping Engineering. Journal of Physical Chemistry Letters, 2022, 13, 3130-3137.	2.1	12
7	Relationship between Carrier Density and Precursor Solution Stirring for Lead-Free Tin Halide Perovskite Solar Cells Performance. ACS Applied Energy Materials, 2022, 5, 4002-4007.	2.5	10
8	Influence of charge transport layer on the crystallinity and charge extraction of pure tin-based halide perovskite film. Journal of Energy Chemistry, 2022, 69, 612-615.	7.1	2
9	Molybdenum Sulfide Quantum Dots Decorated on TiO <sub>2</sub> for Photocatalytic Hydrogen Evolution. ACS Applied Nano Materials, 2022, 5, 702-709.	2.4	8
10	Topâ€Contactsâ€Interface Engineering for Highâ€Performance Perovskite Solar Cell With Reducing Lead Leakage. Solar Rrl, 2022, 6, .	3.1	8
11	Bimetallic oxyhydroxide <i>in situ</i> derived from an Fe <sub>2</sub> Co-MOF for efficient electrocatalytic oxygen evolution. Journal of Materials Chemistry A, 2021, 9, 13271-13278.	5.2	27
12	Electrocatalytic fixation of N <sub>2</sub> into NO <sub>3</sub> <sup>â^'</sup> : electron transfer between oxygen vacancies and loaded Au in Nb <sub>2</sub> O <sub>5â^'<i>x</i></sub> nanobelts to promote ambient nitrogen oxidation. Journal of Materials Chemistry A, 2021, 9, 17442-17450.	5.2	33
13	The role of sodium in stabilizing tin–lead (Sn–Pb) alloyed perovskite quantum dots. Journal of Materials Chemistry A, 2021, 9, 12087-12098.	5.2	9
14	α-Fe <sub>2</sub> O <sub>3</sub> /Ag/CdS ternary heterojunction photoanode for efficient solar water oxidation. Catalysis Science and Technology, 2021, 11, 5859-5867.	2.1	7
15	Modeling of Nucleation and Growth in the Synthesis of PbS Colloidal Quantum Dots Under Variable Temperatures. ACS Omega, 2021, 6, 3701-3710.	1.6	8
16	Study of open circuit voltage loss mechanism in perovskite solar cells. Japanese Journal of Applied Physics, 2021, 60, SBBF13.	0.8	11
17	Relationship between perovsktie solar cell efficiency and lattice disordering. Japanese Journal of Applied Physics, 2021, 60, 035001.	0.8	0
18	Impact of Auger recombination on performance limitation of perovskite solar cell. Solar Energy, 2021, 217, 342-353.	2.9	27

#	Article	IF	CITATIONS
19	Ultra-Halide-Rich Synthesis of Stable Pure Tin-Based Halide Perovskite Quantum Dots: Implications for Photovoltaics. ACS Applied Nano Materials, 2021, 4, 3958-3968.	2.4	9
20	Elegant Construction of ZnIn <sub>2</sub> S <sub>4</sub> /BiVO <sub>4</sub> Hierarchical Heterostructures as Direct Z-Scheme Photocatalysts for Efficient CO <sub>2</sub> Photoreduction. ACS Applied Materials & Interfaces, 2021, 13, 15092-15100.	4.0	115
21	Tinâ€Lead Perovskite Fabricated via Ethylenediamine Interlayer Guides to the Solar Cell Efficiency of 21.74%. Advanced Energy Materials, 2021, 11, 2101069.	10.2	110
22	Passivating Quantum Dot Carrier Transport Layer with Metal Salts. ACS Applied Materials & Interfaces, 2021, 13, 28679-28688.	4.0	3
23	High-Efficiency Lead-Free Wide Band Gap Perovskite Solar Cells via Guanidinium Bromide Incorporation. ACS Applied Energy Materials, 2021, 4, 5615-5624.	2.5	19
24	The effect of water on colloidal quantum dot solar cells. Nature Communications, 2021, 12, 4381.	5.8	44
25	Hollow InVO <sub>4</sub> Nanocuboid Assemblies toward Promoting Photocatalytic N <sub>2</sub> Conversion Performance. Advanced Materials, 2021, 33, e2006780.	11.1	38
26	Resilient Women and the Resiliency of Science. Chemistry of Materials, 2021, 33, 6585-6588.	3.2	3
27	Matrix Manipulation of Directlyâ€Synthesized PbS Quantum Dot Inks Enabled by Coordination Engineering. Advanced Functional Materials, 2021, 31, 2104457.	7.8	24
28	Large Grain Growth and Energy Alignment Optimization by Diethylammonium Iodide Substitution at A Site in Leadâ€Free Tin Halide Perovskite Solar Cells. Solar Rrl, 2021, 5, 2100633.	3.1	14
29	Bismuth Vacancy-Induced Efficient CO <sub>2</sub> Photoreduction in BiOCl Directly from Natural Air: A Progressive Step toward Photosynthesis in Nature. Nano Letters, 2021, 21, 10260-10266.	4.5	74
30	Colloidal quantum-dot bulk-heterojunction solar cells. Journal of Semiconductors, 2021, 42, 110203.	2.0	4
31	Growth of Amorphous Passivation Layer Using Phenethylammonium Iodide for Highâ€Performance Inverted Perovskite Solar Cells. Solar Rrl, 2020, 4, 1900243.	3.1	43
32	Photoexcited hot and cold electron and hole dynamics at FAPbI3 perovskite quantum dots/metal oxide heterojunctions used for stable perovskite quantum dot solar cells. Nano Energy, 2020, 67, 104267.	8.2	35
33	Theoretical analysis of band alignment at back junction in Sn–Ge perovskite solar cells with inverted p-i-n structure. Solar Energy Materials and Solar Cells, 2020, 206, 110268.	3.0	66
34	Reducing trap density and carrier concentration by a Ge additive for an efficient quasi 2D/3D perovskite solar cell. Journal of Materials Chemistry A, 2020, 8, 2962-2968.	5.2	53
35	Effect of Precursor Solution Aging on the Thermoelectric Performance of CsSnI3 Thin Film. Journal of Electronic Materials, 2020, 49, 2698-2703.	1.0	15
36	Photoexcited carrier dynamics in colloidal quantum dot solar cells: insights into individual quantum dots, quantum dot solid films and devices. Chemical Society Reviews, 2020, 49, 49-84.	18.7	70

#	Article	IF	CITATIONS
37	Trioctylphosphine Oxide Acts as Alkahest for SnX <sub>2</sub> /PbX <sub>2</sub> : A General Synthetic Route to Perovskite ASn <sub><i>x</i></sub> Pb <sub>1–<i>x</i></sub> X <sub>3</sub> (A = Cs, FA, MA; X =	) Tj 🖽፬q1	1 0 <b>37</b> 84314 (
38	Inverted CsPbI2Br perovskite solar cells with enhanced efficiency and stability in ambient atmosphere via formamidinium incorporation. Solar Energy Materials and Solar Cells, 2020, 218, 110741.	3.0	21
39	Atomistic and Electronic Origin of Phase Instability of Metal Halide Perovskites. ACS Applied Energy Materials, 2020, 3, 11548-11558.	2.5	23
40	A New Strategy for Increasing the Efficiency of Inverted Perovskite Solar Cells to More than 21%: Highâ€Humidity Induced Selfâ€Passivation of Perovskite Films. Solar Rrl, 2020, 4, 2070094.	3.1	1
41	Passivation Strategy of Reducing Both Electron and Hole Trap States for Achieving High-Efficiency PbS Quantum-Dot Solar Cells with Power Conversion Efficiency over 12%. ACS Energy Letters, 2020, 5, 3224-3236.	8.8	49
42	Surface-Modified Graphene Oxide/Lead Sulfide Hybrid Film-Forming Ink for High-Efficiency Bulk Nano-Heterojunction Colloidal Quantum Dot Solar Cells. Nano-Micro Letters, 2020, 12, 111.	14.4	16
43	Artificial Trees for Artificial Photosynthesis: Construction of Dendrite-Structured α-Fe <sub>2</sub> O <sub>3</sub> /g-C <sub>3</sub> N <sub>4</sub> Z-Scheme System for Efficient CO <sub>2</sub> Reduction into Solar Fuels. ACS Applied Energy Materials, 2020, 3, 6561-6572.	2.5	67
44	Nearâ€Infrared Emission from Tin–Lead (Sn–Pb) Alloyed Perovskite Quantum Dots by Sodium Doping. Angewandte Chemie, 2020, 132, 8499-8502.	1.6	10
45	Enhanced Device Performance with Passivation of the TiO <sub>2</sub> Surface Using a Carboxylic Acid Fullerene Monolayer for a SnPb Perovskite Solar Cell with a Normal Planar Structure. ACS Applied Materials & Interfaces, 2020, 12, 17776-17782.	4.0	24
46	Super stable CsPbBr3@SiO2 tumor imaging reagent by stress-response encapsulation. Nano Research, 2020, 13, 795-801.	5.8	55
47	Nearâ€Infrared Emission from Tin–Lead (Sn–Pb) Alloyed Perovskite Quantum Dots by Sodium Doping. Angewandte Chemie - International Edition, 2020, 59, 8421-8424.	7.2	38
48	In-Depth Exploration of the Charge Dynamics in Surface-Passivated ZnO Nanowires. Journal of Physical Chemistry C, 2020, 124, 15812-15817.	1.5	6
49	All-inorganic cesium lead halide perovskite nanocrystals for solar-pumped laser application. Journal of Applied Physics, 2020, 127, .	1.1	15
50	Exquisite design of porous carbon microtubule-scaffolding hierarchical In <sub>2</sub> O <sub>3</sub> -ZnIn <sub>2</sub> S <sub>4</sub> heterostructures toward efficient photocatalytic conversion of CO <sub>2</sub> into CO. Nanoscale, 2020, 12, 14676-14681.	2.8	31
51	Boosting Photocatalytic CO <sub>2</sub> Reduction on CsPbBr <sub>3</sub> Perovskite Nanocrystals by Immobilizing Metal Complexes. Chemistry of Materials, 2020, 32, 1517-1525.	3.2	197
52	Lead-free tin-halide perovskite solar cells with 13% efficiency. Nano Energy, 2020, 74, 104858.	8.2	347
53	A New Strategy for Increasing the Efficiency of Inverted Perovskite Solar Cells to More than 21%: Highâ€Humidity Induced Selfâ€Passivation of Perovskite Films. Solar Rrl, 2020, 4, 2000149.	3.1	17
54	<i>In situ</i> preparation of Bi <sub>2</sub> S <sub>3</sub> nanoribbon-anchored BiVO <sub>4</sub> nanoscroll heterostructures for the catalysis of Cr( <scp>vi</scp> ) photoreduction. Catalysis Science and Technology, 2020, 10, 3843-3847.	2.1	14

#	Article	IF	CITATIONS
55	Fabrication of Oriented FTO Film Grown By Spray Pyrolysis. ECS Meeting Abstracts, 2020, MA2020-02, 1909-1909.	0.0	0
56	(Invited) Phase Stable and Less-Defect Perovskite Quantum Dots: Optical Property, Photoexcited Carrier Dynamics, and Application to Solar Cells. ECS Meeting Abstracts, 2020, MA2020-02, 1878-1878.	0.0	0
57	Relationship between Lattice Strain and Efficiency for Sn-Perovskite Solar Cells. ACS Applied Materials & Interfaces, 2019, 11, 31105-31110.	4.0	101
58	CsPb(I Br1â^')3 solar cells. Science Bulletin, 2019, 64, 1532-1539.	4.3	114
59	Suppression of Charge Carrier Recombination in Lead-Free Tin Halide Perovskite via Lewis Base Post-treatment. Journal of Physical Chemistry Letters, 2019, 10, 5277-5283.	2.1	196
60	A multi-objective optimization-based layer-by-layer blade-coating approach for organic solar cells: rational control of vertical stratification for high performance. Energy and Environmental Science, 2019, 12, 3118-3132.	15.6	142
61	Strain Relaxation and Light Management in Tin–Lead Perovskite Solar Cells to Achieve High Efficiencies. ACS Energy Letters, 2019, 4, 1991-1998.	8.8	114
62	The Effect of Transparent Conductive Oxide Substrate on the Efficiency of SnGe-perovskite Solar Cells. Journal of Photopolymer Science and Technology = [Fotoporima Konwakai Shi], 2019, 32, 597-602.	0.1	5
63	The interparticle distance limit for multiple exciton dissociation in PbS quantum dot solid films. Nanoscale Horizons, 2019, 4, 445-451.	4.1	19
64	Pb-free Sn Perovskite Solar Cells Doped with Samarium Iodide. Chemistry Letters, 2019, 48, 836-839.	0.7	6
65	Improving Photovoltaic Performance of ZnO Nanowires Based Colloidal Quantum Dot Solar Cells via SnO2 Passivation Strategy. Frontiers in Energy Research, 2019, 7, .	1.2	19
66	Highly symmetrical, 24-faceted, concave BiVO <sub>4</sub> polyhedron bounded by multiple high-index facets for prominent photocatalytic O <sub>2</sub> evolution under visible light. Chemical Communications, 2019, 55, 4777-4780.	2.2	29
67	BiVO <sub>4</sub> tubular structures: oxygen defect-rich and largely exposed reactive {010} facets synergistically boost photocatalytic water oxidation and the selective Nî€N coupling reaction of 5-amino-1 <i>H</i> -tetrazole. Chemical Communications, 2019, 55, 5635-5638.	2.2	17
68	Micro-scale current path distributions of Zn1-Mg O-coated SnO2:F transparent electrodes prepared by sol-gel and sputtering methods in perovskite solar cells. Thin Solid Films, 2019, 669, 455-460.	0.8	5
69	Determination of iron species, including biomineralized jarosite, in the iron-hyperaccumulator moss Scopelophila ligulata by MA¶ssbauer, X-ray diffraction, and elemental analyses. BioMetals, 2019, 32, 171-184.	1.8	1
70	Role of GeI2 and SnF2 additives for SnGe perovskite solar cells. Nano Energy, 2019, 58, 130-137.	8.2	104
71	Gel <sub>2</sub> Additive for High Optoelectronic Quality CsPbl <sub>3</sub> Quantum Dots and Their Application in Photovoltaic Devices. Chemistry of Materials, 2019, 31, 798-807.	3.2	112

52 Surface Coatings for Improving Solar Cell Efficiencies. , 2019, , .

#	Article	IF	CITATIONS
73	Hindered Formation of Photoinactive δ-FAPbl <sub>3</sub> Phase and Hysteresis-Free Mixed-Cation Planar Heterojunction Perovskite Solar Cells with Enhanced Efficiency via Potassium Incorporation. Journal of Physical Chemistry Letters, 2018, 9, 2113-2120.	2.1	72
74	Octadecylamineâ€Functionalized Singleâ€Walled Carbon Nanotubes for Facilitating the Formation of a Monolithic Perovskite Layer and Stable Solar Cells. Advanced Functional Materials, 2018, 28, 1705545.	7.8	73
75	Ultrafast Electron Injection from Photoexcited Perovskite CsPbI <sub>3</sub> QDs into TiO <sub>2</sub> Nanoparticles with Injection Efficiency near 99%. Journal of Physical Chemistry Letters, 2018, 9, 294-297.	2.1	75
76	Highly Efficient 17.6% Tin–Lead Mixed Perovskite Solar Cells Realized through Spike Structure. Nano Letters, 2018, 18, 3600-3607.	4.5	114
77	Understanding charge transfer and recombination by interface engineering for improving the efficiency of PbS quantum dot solar cells. Nanoscale Horizons, 2018, 3, 417-429.	4.1	50
78	Crystal Growth, Exponential Optical Absorption Edge, and Ground State Energy Level of PbS Quantum Dots Adsorbed on the (001), (110), and (111) Surfaces of Rutile-TiO <sub>2</sub> . Journal of Physical Chemistry C, 2018, 122, 13590-13599.	1.5	3
79	Mixed Sn–Ge Perovskite for Enhanced Perovskite Solar Cell Performance in Air. Journal of Physical Chemistry Letters, 2018, 9, 1682-1688.	2.1	206
80	Recombination Suppression in PbS Quantum Dot Heterojunction Solar Cells by Energy-Level Alignment in the Quantum Dot Active Layers. ACS Applied Materials & Interfaces, 2018, 10, 26142-26152.	4.0	24
81	Growth Mechanism of ZnO Thin Films Grown by Spray Pyrolysis Using Diethylzinc Solution. Physica Status Solidi (A) Applications and Materials Science, 2018, 215, 1700406.	0.8	2
82	Construction of Al-ZnO/CdS photoanodes modified with distinctive alumina passivation layer for improvement of photoelectrochemical efficiency and stability. Nanoscale, 2018, 10, 19621-19627.	2.8	16
83	Anisotropic Crystal Growth, Optical Absorption, and Ground-State Energy Level of CdSe Quantum Dots Adsorbed on the (001) and (102) Surfaces of Anatase-TiO <sub>2</sub> : Quantum Dot-Sensitization System. Journal of Physical Chemistry C, 2018, 122, 29200-29209.	1.5	3
84	Two-Step Synthesis of Laminar Vanadate via a Facile Hydrothermal Route and Enhancing the Photocatalytic Reduction of CO <sub>2</sub> into Solar Fuel through Tuning of the Oxygen Vacancies by in Situ Vacuum Illumination Treatment. ACS Applied Energy Materials, 2018, 1, 6857-6864.	2.5	9
85	New Tin(II) Fluoride Derivative as a Precursor for Enhancing the Efficiency of Inverted Planar Tin/Lead Perovskite Solar Cells. Journal of Physical Chemistry C, 2018, 122, 27284-27291.	1.5	26
86	Allâ€Inorganic CsPb <sub>1â^'<i>x</i></sub> Ge <sub><i>x</i></sub> I <sub>2</sub> Br Perovskite with Enhanced Phase Stability and Photovoltaic Performance. Angewandte Chemie, 2018, 130, 12927-12931.	1.6	31
87	Allâ€Inorganic CsPb <sub>1â^'<i>x</i></sub> Ge <sub><i>x</i></sub> I <sub>I<sub>Br Perovskite with Enhanced Phase Stability and Photovoltaic Performance. Angewandte Chemie - International Edition, 2018, 57, 12745-12749.</sub></sub>	7.2	157
88	Interface Passivation Effects on the Photovoltaic Performance of Quantum Dot Sensitized Inverse Opal TiO2 Solar Cells. Nanomaterials, 2018, 8, 460.	1.9	20
89	Effect of the conduction band offset on interfacial recombination behavior of the planar perovskite solar cells. Nano Energy, 2018, 53, 17-26.	8.2	110
90	Lead Selenide Colloidal Quantum Dot Solar Cells Achieving High Open-Circuit Voltage with One-Step Deposition Strategy, Journal of Physical Chemistry Letters, 2018, 9, 3598-3603	2.1	38

#	Article	IF	CITATIONS
91	Solutionâ€Processed Airâ€Stable Copper Bismuth Iodide for Photovoltaics. ChemSusChem, 2018, 11, 2930-2935.	3.6	39
92	Alloying Strategy in Cu–In–Ga–Se Quantum Dots for High Efficiency Quantum Dot Sensitized Solar Cells. ACS Applied Materials & Interfaces, 2017, 9, 5328-5336.	4.0	87
93	Improvement of Photovoltaic Performance of Colloidal Quantum Dot Solar Cells Using Organic Small Molecule as Hole-Selective Layer. Journal of Physical Chemistry Letters, 2017, 8, 2163-2169.	2.1	35
94	Ligand-dependent exciton dynamics and photovoltaic properties of PbS quantum dot heterojunction solar cells. Physical Chemistry Chemical Physics, 2017, 19, 6358-6367.	1.3	31
95	High Efficiency Quantum Dot Sensitized Solar Cells Based on Direct Adsorption of Quantum Dots on Photoanodes. ACS Applied Materials & Interfaces, 2017, 9, 22549-22559.	4.0	39
96	Investigation of Interfacial Charge Transfer in Solution Processed Cs <sub>2</sub> SnI <sub>6</sub> Thin Films. Journal of Physical Chemistry C, 2017, 121, 13092-13100.	1.5	66
97	Dependences of the Optical Absorption, Ground State Energy Level, and Interfacial Electron Transfer Dynamics on the Size of CdSe Quantum Dots Adsorbed on the (001), (110), and (111) Surfaces of Single Crystal Rutile TiO <sub>2</sub> . Journal of Physical Chemistry C, 2017, 121, 25390-25401.	1.5	6
98	Colloidal Synthesis of Air-Stable Alloyed CsSn <sub>1–<i>x</i></sub> Pb <sub><i>x</i></sub> I <sub>3</sub> Perovskite Nanocrystals for Use in Solar Cells. Journal of the American Chemical Society, 2017, 139, 16708-16719.	6.6	314
99	Slow hot carrier cooling in cesium lead iodide perovskites. Applied Physics Letters, 2017, 111, .	1.5	56
100	Copper deficient Zn–Cu–In–Se quantum dot sensitized solar cells for high efficiency. Journal of Materials Chemistry A, 2017, 5, 21442-21451.	5.2	73
101	Hole-Transport Materials Containing Triphenylamine Donors with a Spiro[fluorene-9,9′-xanthene] Core for Efficient and Stable Large Area Perovskite Solar Cells (Solar RRL 9â^•2017). Solar Rrl, 2017, 1, 1770134.	3.1	3
102	Highly Luminescent Phase-Stable CsPbI <sub>3</sub> Perovskite Quantum Dots Achieving Near 100% Absolute Photoluminescence Quantum Yield. ACS Nano, 2017, 11, 10373-10383.	7.3	748
103	A 2,1,3-Benzooxadiazole Moiety in a D–A–D-type Hole-Transporting Material for Boosting the Photovoltage in Perovskite Solar Cells. Journal of Physical Chemistry C, 2017, 121, 17617-17624.	1.5	40
104	Hole-Transport Materials Containing Triphenylamine Donors with a Spiro[fluorene-9,9′-xanthene] Core for Efficient and Stable Large Area Perovskite Solar Cells. Solar Rrl, 2017, 1, 1700096.	3.1	19
105	Femtosecond dynamics of optical nonlinearities in nanocomposite films highly dispersed with semiconductor CdSe quantum dots. , 2017, , .		0
106	Optimization of Experimental Parameters for the Performance of Solid-state Dye-sensitized Solar Cells. Analytical Sciences, 2017, 33, 1041-1046.	0.8	3
107	Air Stable PbSe Colloidal Quantum Dot Heterojunction Solar Cells: Ligand-Dependent Exciton Dissociation, Recombination, Photovoltaic Property, and Stability. Journal of Physical Chemistry C, 2016, 120, 28509-28518.	1.5	45
108	The effect of CdS on the charge separation and recombination dynamics in PbS/CdS double-layered quantum dot sensitized solar cells. Chemical Physics, 2016, 478, 159-163.	0.9	10

#	Article	IF	CITATIONS
109	Surface engineering of PbS quantum dot sensitized solar cells with a conversion efficiency exceeding 7%. Journal of Materials Chemistry A, 2016, 4, 7214-7221.	5.2	101
110	Recent progress on quantum dot solar cells: a review. Journal of Photonics for Energy, 2016, 6, 040901.	0.8	60
111	Architecture of the Interface between the Perovskite and Holeâ€Transport Layers in Perovskite Solar Cells. ChemSusChem, 2016, 9, 2634-2639.	3.6	27
112	Facile Synthesis and Characterization of Sulfur Doped Low Bandgap Bismuth Based Perovskites by Soluble Precursor Route. Chemistry of Materials, 2016, 28, 6436-6440.	3.2	87
113	Thiocyanate-free asymmetric ruthenium(II) dye sensitizers containing azole chromophores with near-IR light-harvesting capacity. Journal of Power Sources, 2016, 331, 100-111.	4.0	16
114	Adsorption and Electronic Structure of CdSe Quantum Dots on Single Crystal ZnO: A Basic Study of Quantum Dot-Sensitization System. Journal of Physical Chemistry C, 2016, 120, 16367-16376.	1.5	11
115	The Electronic Structure and Photoinduced Electron Transfer Rate of CdSe Quantum Dots on Single Crystal Rutile TiO <sub>2</sub> : Dependence on the Crystal Orientation of the Substrate. Journal of Physical Chemistry C, 2016, 120, 2047-2057.	1.5	22
116	Neutral and anionic tetrazole-based ligands in designing novel ruthenium dyes for dye-sensitized solar cells. Journal of Power Sources, 2016, 307, 416-425.	4.0	27
117	Mn doped quantum dot sensitized solar cells with power conversion efficiency exceeding 9%. Journal of Materials Chemistry A, 2016, 4, 877-886.	5.2	122
118	Zn–Cu–In–Se Quantum Dot Solar Cells with a Certified Power Conversion Efficiency of 11.6%. Journal of the American Chemical Society, 2016, 138, 4201-4209.	6.6	537
119	CdSeTe/CdS Type-I Core/Shell Quantum Dot Sensitized Solar Cells with Efficiency over 9%. Journal of Physical Chemistry C, 2015, 119, 28800-28808.	1.5	131
120	High reduction of interfacial charge recombination in colloidal quantum dot solar cells by metal oxide surface passivation. Nanoscale, 2015, 7, 5446-5456.	2.8	82
121	Electronic structures of two types of TiO <sub>2</sub> electrodes: inverse opal and nanoparticulate cases. RSC Advances, 2015, 5, 49623-49632.	1.7	26
122	Optical absorption, charge separation and recombination dynamics in Sn/Pb cocktail perovskite solar cells and their relationships to photovoltaic performances. Journal of Materials Chemistry A, 2015, 3, 9308-9316.	5.2	85
123	Uncovering the charge transfer and recombination mechanism in ZnS-coated PbS quantum dot sensitized solar cells. Solar Energy, 2015, 122, 307-313.	2.9	19
124	Characterization of hot carrier cooling and multiple exciton generation dynamics in PbS QDs using an improved transient grating technique. Journal of Energy Chemistry, 2015, 24, 712-716.	7.1	9
125	All-Solid Perovskite Solar Cells with HOCO-R-NH <sub>3</sub> <sup>+</sup> I <sup>–</sup> Anchor-Group Inserted between Porous Titania and Perovskite. Journal of Physical Chemistry C, 2014, 118, 16651-16659.	1.5	191
126	Ex Situ CdSe Quantum Dot-Sensitized Solar Cells Employing Inorganic Ligand Exchange To Boost Efficiency. Journal of Physical Chemistry C, 2014, 118, 214-222.	1.5	44

#	Article	IF	CITATIONS
127	Influence of linker molecules on interfacial electron transfer and photovoltaic performance of quantum dot sensitized solar cells. Journal of Materials Chemistry A, 2014, 2, 20882-20888.	5.2	52
128	Role of lithium and co-existing cations in electrolyte to improve performance of dye-sensitized solar cells. RSC Advances, 2014, 4, 21517-21520.	1.7	14
129	Effect of TiO2 Crystal Orientation on the Adsorption of CdSe Quantum Dots for Photosensitization Studied by the Photoacoustic and Photoelectron Yield Methods. Journal of Physical Chemistry C, 2014, 118, 16680-16687.	1.5	10
130	Charge transfer and recombination at the metal oxide/CH <sub>3</sub> NH <sub>3</sub> PbClI <sub>2</sub> /spiro-OMeTAD interfaces: uncovering the detailed mechanism behind high efficiency solar cells. Physical Chemistry Chemical Physics, 2014, 16, 19984-19992.	1.3	88
131	High-Efficiency "Green―Quantum Dot Solar Cells. Journal of the American Chemical Society, 2014, 136, 9203-9210.	6.6	547
132	CH <sub>3</sub> NH <sub>3</sub> Sn <sub><i>x</i></sub> Pb <sub>(1–<i>x</i>)</sub> I <sub>3</sub> Perovskite Solar Cells Covering up to 1060 nm. Journal of Physical Chemistry Letters, 2014, 5, 1004-1011.	2.1	852
133	Huge suppression of charge recombination in P3HT–ZnO organic–inorganic hybrid solar cells by locating dyes at the ZnO/P3HT interfaces. Physical Chemistry Chemical Physics, 2013, 15, 14370.	1.3	33
134	Carrier dynamics in quantum-dot sensitized solar cells measured by transient grating and transient absorption methods. Physical Chemistry Chemical Physics, 2013, 15, 11006.	1.3	18
135	Optical absorption of CdSe quantum dots on electrodes with different morphology. AIP Advances, 2013, 3, 102115.	0.6	12
136	Effect of ZnS coatings on the enhancement of the photovoltaic properties of PbS quantum dot-sensitized solar cells. Journal of Applied Physics, 2012, 111, .	1.1	66
137	Multiple electron injection dynamics in linearly-linked two dye co-sensitized nanocrystalline metal oxide electrodes for dye-sensitized solar cells. Physical Chemistry Chemical Physics, 2012, 14, 4605.	1.3	35
138	Quantum-Dot-Sensitized Solar Cells: Effect of Nanostructured TiO <sub>2</sub> Morphologies on Photovoltaic Properties. Journal of Physical Chemistry Letters, 2012, 3, 1885-1893.	2.1	101
139	Ultrafast carrier dynamics in PbS quantum dots. Chemical Physics Letters, 2012, 542, 89-93.	1.2	26
140	Effect of nanostructured electrode architecture and semiconductor deposition strategy on the photovoltaic performance of quantum dot sensitized solar cells. Electrochimica Acta, 2012, 75, 139-147.	2.6	62
141	Dependences of the optical absorption and photovoltaic properties of CdS quantum dot-sensitized solar cells on the CdS quantum dot adsorption time. Journal of Applied Physics, 2011, 110, .	1.1	25
142	Uncovering the role of the ZnS treatment in the performance of quantum dot sensitized solar cells. Physical Chemistry Chemical Physics, 2011, 13, 12024.	1.3	217
143	Highly efficient CdS/CdSe-sensitized solar cells controlled by the structural properties of compact porous TiO2 photoelectrodes. Physical Chemistry Chemical Physics, 2011, 13, 4659.	1.3	271
144	Direct Correlation between Ultrafast Injection and Photoanode Performance in Quantum Dot Sensitized Solar Cells. Journal of Physical Chemistry C, 2010, 114, 22352-22360.	1.5	97

#	Article	IF	CITATIONS
145	CdSe quantum dot-sensitized solar cell employing TiO2 nanotube working-electrode and Cu2S counter-electrode. Applied Physics Letters, 2010, 97, .	1.5	118
146	Sensitization of Titanium Dioxide Photoanodes with Cadmium Selenide Quantum Dots Prepared by SILAR: Photoelectrochemical and Carrier Dynamics Studies. Journal of Physical Chemistry C, 2010, 114, 21928-21937.	1.5	120
147	Separation of ultrafast photoexcited electron and hole dynamics in CdSe quantum dots adsorbed onto nanostructured TiO2 films. Applied Physics Letters, 2010, 97, .	1.5	30
148	Photoacoustic and photoelectrochemical current spectra of combined CdS/CdSe quantum dots adsorbed on nanostructured TiO2 electrodes, together with photovoltaic characteristics. Journal of Applied Physics, 2010, 108, .	1.1	39
149	Photoacoustic spectra of Au quantum dots adsorbed on nanostructured TiO2 electrodes together with the photoelectrochemical current characteristics. Journal of Applied Physics, 2009, 105, .	1.1	29
150	Recombination in Quantum Dot Sensitized Solar Cells. Accounts of Chemical Research, 2009, 42, 1848-1857.	7.6	747
151	Improving the performance of colloidal quantum-dot-sensitized solar cells. Nanotechnology, 2009, 20, 20, 295204.	1.3	383
152	Characterization of electron transfer from CdSe quantum dots to nanostructured TiO2 electrode using a near-field heterodyne transient grating technique. Thin Solid Films, 2008, 516, 5927-5930.	0.8	68
153	Effect of ZnS coating on the photovoltaic properties of CdSe quantum dot-sensitized solar cells. Journal of Applied Physics, 2008, 103, .	1.1	369
154	Crystal Growth of CdSe Quantum Dots Adsorbed on Nanoparticle, Inverse Opal, and Nanotube TiO <sub>2</sub> Photoelectrodes Characterized by Photoacoustic Spectroscopy. Japanese Journal of Applied Physics, 2007, 46, 4616.	0.8	22
155	High efficiency of CdSe quantum-dot-sensitized TiO2 inverse opal solar cells. Applied Physics Letters, 2007, 91, .	1.5	442
156	Optical absorption, photosensitization, and ultrafast carrier dynamic investigations of CdSe quantum dots grafted onto nanostructured SnO2 electrode and fluorine-doped tin oxide (FTO) glass. Chemical Physics Letters, 2007, 442, 89-96.	1.2	51
157	Optical absorption and ultrafast carrier dynamics characterization of CdSe quantum dots deposited on different morphologies of nanostructured TiO2 films. Materials Science and Engineering C, 2007, 27, 1514-1520.	3.8	37
158	Photoacoustic and Photoelectrochemical Characterization of Inverse Opal TiO2Sensitized with CdSe Quantum Dots. Japanese Journal of Applied Physics, 2006, 45, 5563-5568.	0.8	41
159	Photosensitization of nanostructured TiO2 with CdSe quantum dots: effects of microstructure and electron transport in TiO2 substrates. Journal of Photochemistry and Photobiology A: Chemistry, 2004, 164, 75-80.	2.0	130
160	Characterization of Nanostructured TiO2Electrodes Sensitized with CdSe Quantum Dots Using Photoacoustic and Photoelectrochemical Current Methods. Japanese Journal of Applied Physics, 2004, 43, 2946-2951.	0.8	67
161	Synthesis, optical property and photoexcited carrier dynamics of phase stable and less-defect perovskite quantum dots. , 0, , .		0